J Electr Eng Technol.2018; 13(4): 1638-1643
http://doi.org/10.5370/JEET.2018.13.4.1638

ISSN(Print) 1975-0102
ISSN(Online) 2093-7423

Electrical Properties of $BaTiO_3$-based 0603/0.1μF/0.3mm Ceramics Decoupling Capacitor for Embedding in the PCB of 10G RF Transceiver Module

Hwa-sun Park*, Youngil Na*, Ho Joon Choi*, Su-jeong Suh*, Dong-Hyun Baek and Jung-Rag Yoon†**

Abstract – Multi-layer ceramic capacitors as decoupling capacitor were fabricated by dielectric composition with a high dielectric constant. The fabricated decoupling capacitors were embedded in the PCB of the 10G RF transceiver module and evaluated for the characteristics of electrical noise by the level of AC input voltage. In order to further improve the electrical properties of the $BaTiO_3$ based composite, glass frit, MgO, Y_2O_3, Mn_3O, V_2O_5, $BaCO_3$, SiO_2, and Al_2O_3 were used as additives. The electrical properties of the composites were determined by various amounts of additives and optimum sintering temperature. As a result of the optimized composite, it was possible to obtain a density of 5.77g/cm^3, a dielectric constant of 1994, and an insulation resistance of $2.91 \times 10^{12}\ \Omega$ at an additive content of 5wt% and a sintering temperature of 1250ºC. After forming a 2.5μm green sheet using the doctor blade method, a total of 77 layers were laminated and sintered at 1180 ºC. A decoupling capacitor with a size of 0.6 mm (W) × 0.3 mm (L) × 0.3 mm (T) (width, length and thickness, respectively) and a capacitance of 100 nF was embedded using a PCB process for the 10G RF Transceiver modules. In the range of AC input voltage 400mmV @ 500kHz to 2200mV @ 900kHz, the embedded 10G RF Transceiver modules evaluated that it has better electrical performance than the non-embedded modules.

Keywords: Embedded PCB, Decoupling capacitor, $BaTiO_3$, Dielectric properties, RF transceiver module.

1. Introduction

With the development of modern electronics, other related industries such as telecommunications and IoT (Internet of things) are growing rapidly. As communication devices such as smart phones are improved to become low-power, multifunctional, and high-speed devices, efforts are being made to reduce the influence of high-frequency noise generated in the AP (application processor). In order to reduce the noise due to high frequency, there is a tendency to embedding R, L and C passive elements and active device chips in the PCB substrate as shown in Fig. 1. [1] Particularly, passive devices, which occupy more than 50% of the total electronic circuit area, have mounted discrete chip resistors or discrete chip capacitors on the surface of the PCBs. Recently, PCBs incorporating passive elements such as resistors or capacitors are being developed on demand. [2] The optical transceiver module converts the optical signal into an electrical signal from an optical communication system such as a large-capacity router. The optical transceiver module consists of many components, including the LD driver, preamplifier, and passive components. [8] In an environment using high frequency, the optical transceiver is very sensitive to electrical noise. This is because it uses a lot of parts on the PCB, which has a big influence on the high frequency.

In this study, a decoupling capacitor with a multilayer ceramic capacitor (MLCC) structure was fabricated using the optimized $BaTiO_3$ composition in sintering conditions and electrical characteristics were investigated. The

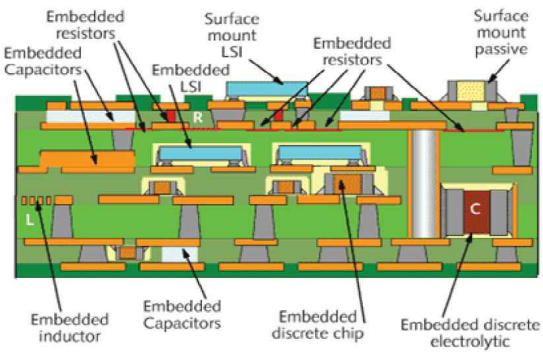

Fig. 1. Schematic diagram of embedding technologies inside a PCB

† Corresponding Author: R&D Center, Samwha Capacitor, Korea. (yoonjungrag@yahoo.co.kr)
* Dept. Advanced Materials Science Engineering, Sungkyunkwan University, Korea. (hspark@skku.edu)
** Dept. of Fire & Disaster Protection Engineering at Gachon University, Korea. (bulbaek@hanmail.net)
Received: May 22, 2017; Accepted: February 5, 2018

fabricated decoupling capacitor has a size of 0.6mm(W) × 0.3mm(L) × 0.3mm(T), a capacitance of 100nF and a temperature characteristic of X5R. It used Ni as the internal electrode and Cu as an external electrode. 10G RF transceiver modules using the fabricated decoupling capacitors were fabricated by the embedding PCB process such as lamination, via processing, plating and circuit formation. To improve the properties of electrical noise, the decoupling capacitor was placed directly beneath the IC terminal, which plays an important role in the 10G RF transceiver modules, to minimize the length of the electrical circuit. And 10G RF transceiver module fabricated by embedded PCB were measured the characteristics of the electrical noise and evaluated that it has better electrical performance than the non-embedded product.

2. Experimental Details

2.1 Fabrication of decoupling capacitor with a structure of MLCC

A $BaTiO_3$ powder (size: 170 nm) that was prepared by the hydrothermal method was used to fabricate a ceramic capacitor. Glass frit, MgO, Y_2O_3, Mn_3O, V_2O_5, $BaCO_3$, SiO_2 and Al_2O_3 were added to inhibit grain growth, accelerate low-temperature sintering, reduce resistance and improve reliability.

Zirconia balls and law materials were added according to the compositions and mixed and pulverized using a bead mill for 24 hours. MLCC were fabricated using a multilayer chip ceramic process described in detail elsewhere. [6,7] The slurry for the preparation of the green sheet was mixed with the ceramic raw materials, dispersing agents and solvent (toluene / ethanol) at an appropriate ratio and then mixed and dispersed for 8 hours using a basket mill. The slurry was further processed by adding PVB (Sekisui, BM-SZ) and DOP (DC chemical) to the mixed and dispersed slurry in an appropriate blending ratio for 4 hours, and a 2.5 μm green sheet was then formed using the doctor blade method. The green sheet was then printed with Ni paste, and 77 layers were laminated, followed by compression and cutting to produce a laminated chip having dimensions of 0.6x0.3x0.3mm. The laminated chips were degreased at 250 °C for 48 hours and then fired at 1140 °C, 1160 °C and 1180 °C for 2 hours under H_2 partial pressures of 10-11 MPa using a mixture of H_2-N_2-H_2O gases. To improve the reliability of MLCC, the reformation heat treatment was performed at 900 °C and $PO_2 = 10^{-7}$ MPa for 2 hours. The external electrodes were fired using a Cu electrode after polishing so that the internal electrodes were left out of the fired chip. The dielectric property was measured at 1 kHz and 1Vrms using an LCR meter (HP4278A, HP, USA). Insulation resistance was measured with a high resistance meter (HP4339B, HP, USA).

2.2 Fabrication of a 10G RF transceiver module

The 10G RF transceiver module is designed to embedding the 0603 MLCC (capacitance: 100nF, thickness: 0.3mm) in the PCB. MLCC as decoupling capacitor were embedded in 2-3 layers and 5-6 layers with 6 layer of PCB and the total thickness of about 1mm. The size of 0.6mm(W) × 0.3mm(L) × 0.3mm(T) were embedded by using PCB process in sequence such as lamination, via processing, plating and circuit formation. [9] To improve the properties of electrical noise in high frequency, MLCC was placed directly beneath the IC terminal, which plays an important role in the 10G RF transceiver modules, to minimize the length of the electrical circuit. The external electrode of the MLCC was coated with a Cu material, and its width was 300μm and its length was 200μm. Via was formed by using CO_2 laser to electrically connect to external IC from embedded MLCC in PCB. The size of a formed via is 100μm on the top and 70μm on the bottom. To fill cu in the formed via, via were filled using electroless/electrolytic plating. Thus, the embedded MLCC is electrically connected to the outermost layer of the PCB and can be used as a passive component on the module. In order to operate a 10G RF transceiver module electrically, other passive components and active components was equipped on the 1st and 6th layers of PCB using the SMT process.

3. Results and Discussion

3.1 Dielectric properties according to additive and sintering temperature

Fig. 2 shows the XRD results with various amounts of additive at a sintering temperature of 1260 °C. As the proportion of additives increases, the main peak shifts slightly to a higher angle. The shift of the main peak to the higher angle is likely due to the increase in the lattice volume of the pseudo-cubic crystal phase as the additive

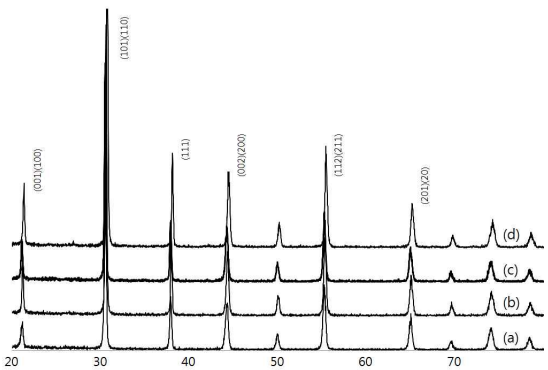

Fig. 2. XRD patterns of $BaTiO_3$ specimens with various additive contents: (a) 3 wt.%; (b) 4 wt.%; (c) 5 wt.%; (d) 6 wt.%.

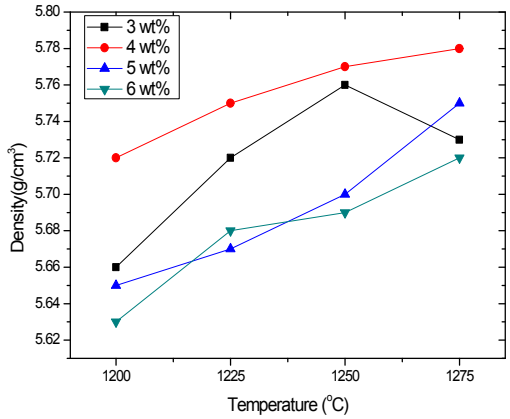

Fig. 3. Bulk Density of $BaTiO_3$ specimens as a function of additive contents and sintering temperature

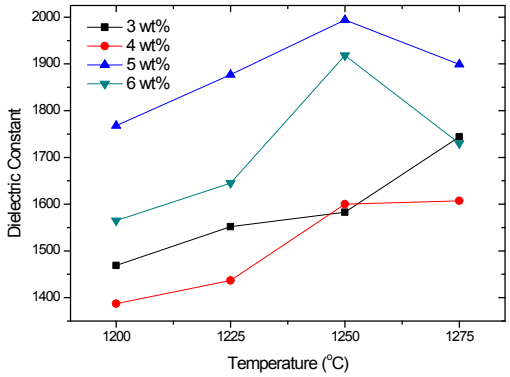

Fig. 4. Dielectric constant of $BaTiO_3$ specimens as a function of additive contents and sintering temperature

diffuses into the cubic + tetragonal structure of $BaTiO_3$.

Fig. 3 shows the density as a function of additive content and sintering temperature. As the proportion of the additive increases from 3 to 4 wt%, the density increases, but when the proportion of the additive is increased to 5 and 6 wt%, the density decreases. The density tends to increase with increasing sintering temperature regardless of the amount of additive. Therefore, although the density is affected by the temperature, there is no significant influence depending on the proportion of the additive. Fig. 4 shows the dielectric constant of the sample with respect to the additive content and sintering temperature. It can be seen that a change in dielectric constant with sintering temperature is similar to that seen at density in Fig. 3. On the other hand, the dielectric constant increases as the proportion of the additive increases. This phenomenon is due to the increased presence of additives in the core shell structure.

Fig. 5 shows the insulation resistance as a function of additive content and sintering temperature. At 1200 °C, the specimens showed low insulation resistance due to the decrease in sintering density, and insulation is well known to be affected by the crystal phase and sinterability of

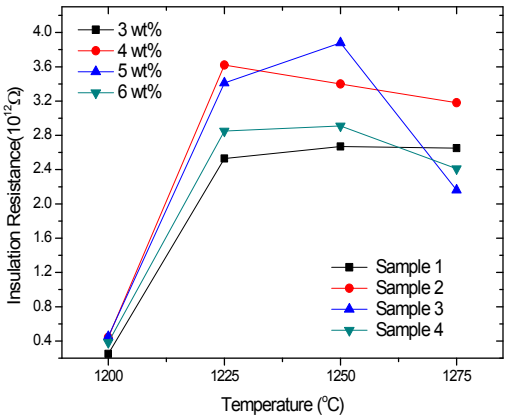

Fig. 5. Insulation resistance as a function of additive content and sintering temperature

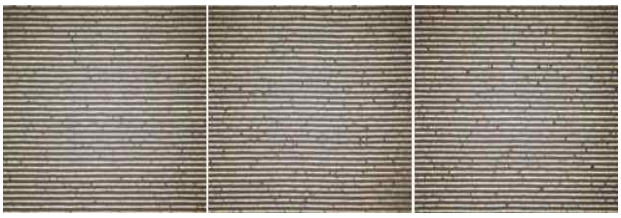

Fig. 6. Optical image of MLCC as a function of sintering temperature

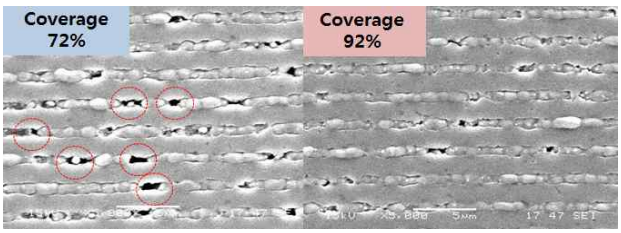

Fig. 7. SEM image of MLCC as a function of sintering temperature (a) 1140 °C and (b) 1160 °C

$BaTiO_3$.[10] Above 1225 °C, the insulation resistance was more than 1×10^{12} Ω as expected due to the compensation of the atoms by the additive.[11]

3.2 Characteristics of decoupling capacitor with a structure of MLCC

Fig. 6 is an optical microscope photograph of a multilayer ceramic chip capacitor produced by forming a green chip having $BaTiO_3$ as a main component and having an added amount of 4 wt%. The sintering temperatures are 1140 °C (a), 1160 °C (b) and 1180 °C (c). It can be seen that the electrode coverage rate increases with increasing sintering temperature. As seen in the 1180 °C image, a broken electrode is observed.

Fig. 7 shows a cross section of a multilayer chip ceramic capacitor by an electron microscope (SEM). The electrode coverage rate at 1140 °C is 72% and increased to 92% at 1160 °C. Fig. 8 is a photograph of the internal cross-

sectional structure of a multilayer ceramic capacitor obtained by baking at 1160 °C and 1180 °C with $BaTiO_3$ as a main component and adding 4 wt% of additives. As shown in the microstructure, the particle size is 150 to 400 μm, and uniform internal and external electrodes are shown.

3.3 Noise characteristics of 10 G RF transceiver module

Fig. 9 is a circuit diagram designed to embedding MLCC with 0603 size and 0.3mm thickness, 100 nF capacitance in the PCB inner layer. The embedding position of the MLCC on modules is shown.

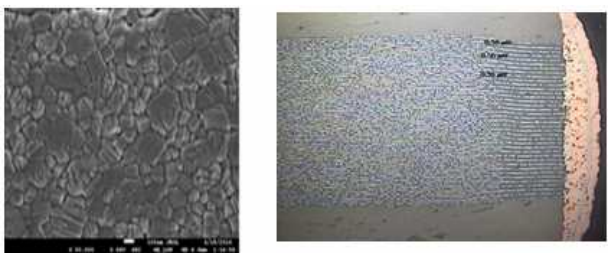

Fig. 8. Sectional SEM image of MLCC

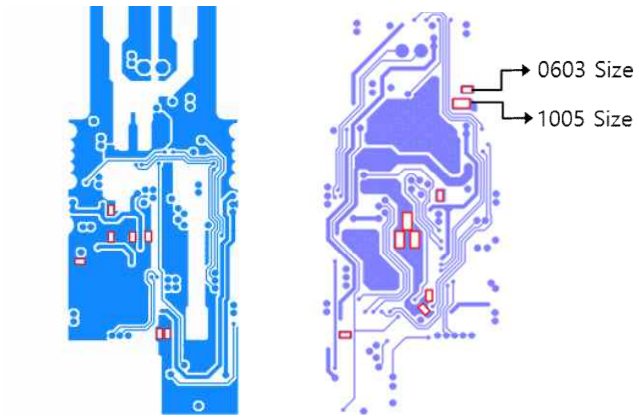

(a) (b)

Fig. 9. Embedded location of decoupling capacitor in 6-layer PCB. (a) L2-L3 Layer (b) L4-L5 Layer

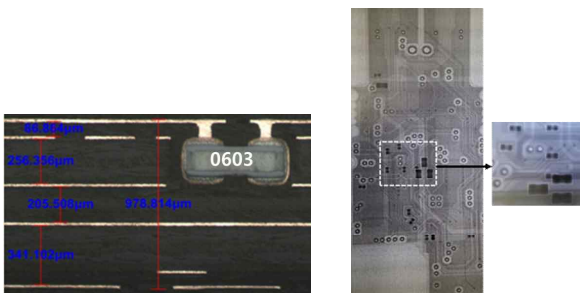

(a) (b)

Fig. 10. Cross-section and X-ray picture of the embedded decoupling capacitor in 6-layer PCB. (a) Single-sided photograph (b) X-ray photograph

Fig. 10 shows a cross-section and an X-ray image for the embedded MLCC in a 1mm of PCB thickness. Fig. 11 shows a fabricated 10G RF transceiver module with dimensions of 330 × 250mm. The IC and the passive components are mounted on embedded PCB by SMT processing. On the front, there is an MCU that can control the transmitter and receiver. On the rear, there is a circuit that can operate the transmitter and the receiver.

Fig. 11(a) consists of a circuit for driving the transmitter and the receiver. Fig. 11(b) shows the MCU attached to control the module. To match the circuit to the 10G signal frequency, the I/O terminal circuit has an impedance match of 50 Ω.

Fig. 12 shows the AC input voltage (mmVp-p) depending on the frequency for the MLCC embedded and non-embedded 10G transceiver modules. A high value of voltage o AC level means that there is more noise on the input power supply. A large value of the measured input noise means that the module operates normally up to the AC input voltage of the measured electrical noise. Therefore, by applying AC input voltage as noise to the input of the module, it is possible to evaluate the performance of the product whether the 10G Transceiver

Fig. 11. Photo of a fabricated 10G RF transceiver modules: (a) Transmitter and receiver plane pictures (top side of the circuit); (b) MCU plane picture (bottom side of the circuit)

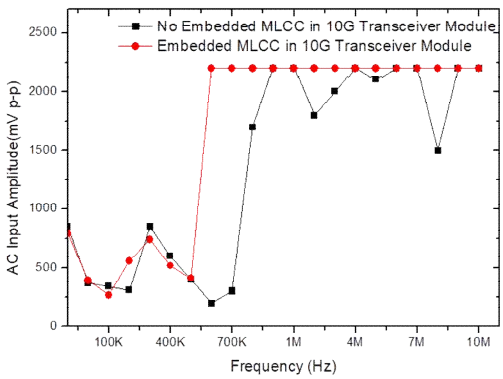

Fig. 12. AC input voltage according to frequency for embedded decoupling capacitor and non-embedded PCB

module operates normally or abnormally at an arbitrary input voltage. In the range of AC input voltage 400mmV @ 500kHz to 2200mV @ 900kHz, the embedded module evaluated that it has better electrical performance than the non-embedded product. [12,13]

4. Conclusion

In this study, A $BaTiO_3$ powder (size:170nm) that was prepared by the hydrothermal method was used to fabricate a ceramic capacitor. Glass frit, MgO, Y_2O_3, Mn_3O, V_2O_5, $BaCO_3$, SiO_2 and Al_2O_3 were added to inhibit grain growth, accelerate low-temperature sintering, reduce resistance and improve reliability. The shift of the main peak to the higher angle is likely due to the increase in the lattice volume of the pseudo-cubic crystal phase as the additive diffuses into the cubic + tetragonal structure of $BaTiO_3$. The density tends to increase with increasing sintering temperature regardless of the amount of additive. Therefore, although the density is affected by the temperature, there is no significant influence depending on the proportion of the additive. The dielectric constant increases as the proportion of the additive increases. This phenomenon is due to the increased presence of additives in the core shell structure. At 1200°C, the specimens showed low insulation resistance due to the decrease in sintering density, and insulation is well known to be affected by the crystal phase and sinterability of BaTiO3. Above 1225°C, the insulation resistance was more than $1\times10^{12}\Omega$ as expected due to the compensation of the atoms by the additive.

Therefore, the fabricated MLCC is applied as a structure optimized for embedded PCB. Embedded MLCC using the process of the embedded PCB for 10 RF transceiver modules has reduced the circuit length to IC compared to circuit length of existing SMT parts. As a result, the embedded and fabricated modules evaluated that they have better electrical performance than the non-embedded products in the AC input voltage range of 400mV @ 500 kHz to 2200mV @ 900kHz.

Acknowledgements

1) This research was supported by Basic Science Research Program through the National Research Foundation of Korea(NRF) funded by the Ministry of Education(NRF-2016R1A6A3A11931569).

2) This study was supported by GRRC program of Gyeonggi Province (GRRC Sungkyunkwan 2017-B02: Development of MEMS-based ultra-thin & ultra-thin temperature / humidity / pressure convergence environment sensor) which is funded by Material & Process Platform for Convergence Sensors.

3) We would like to acknowledge the financial support from the R&D Convergence Program of MSIP (Ministry of Science, ICT and Future Planning) and NST (National Research Council of Science & Technology) of Republic Korea (Grant CAP-13-02-ETRI).

References

[1] Radim Uher, Tomas Zednicek, http://www.avx.com

[2] Jung-Rag Yoon, Jeong-Woo Han, and Kyung-Min Lee, "Dielectric Properties of Polymer-ceramic Composites for Embedded Capacitors," *Trans. Electr. Electron. Mater*., vol. 10, no. 4, pp. 116-120, August 2009.

[3] R. R. Tummala, M. Swaminathan, M. M. Tentzeris, J. Laskar, G. K. Chang, S. Sitaraman, D. Keezer, D. Guidotti, Z. Huang, K. Lim, L. Wan, S. K. Bhattacharya, V. Sundaram, F. Liu, and P. M. Raj, "The SOP for miniaturized, mixed-signal computing, communication, and consumer systems of the next decade," *IEEE Trans. Adv.,* vol. 27 , issue 2, pp. 250-267, September 2004.

[4] J. R. Yoon, B. H. Moon, H. Y. Lee, D. Y. Jeong, D. H. Rhie, "Design and Analysis of Electrical Properties of a Multilayer Ceramic Capacitor Module for DC-Link of Hybrid Electric Vehicles," *J. Electr. Eng. Technol.,* vol. 8, no.4, pp.808-812, July 2013.

[5] Seung-Hwan Lee, Dae-Young Kim, Min-Kee Kim, Hong-Ki Kim, Jeong Hyun Lee, Esther Baek and Jung-Rag Yoon, "Electrical properties of Dy-doped BaTiO3-based Ceramics for MLCC," *Journal of Ceramic Processing Research*, vol. 16, no. 5, pp.495-498 , 2015.

[6] D. Y. Jeong, S. I. Lee, H. Y. Lee, M. K. Kim and Jung-Rag Yoon, "Electrical Properties of $BaTiO_3$-Based Multilayer Ceramic Capacitors Sintered with Plasma-Treated Glass Powder," *Jpn. J. Appl. Phys*., vol. 52, no. 10s, October 2013.

[7] Mikko Karppinen, et al., "Parallel Optical Interconnect between Ceramic BGA Packages on FR4 Board using Embedded Waveguides and Passive Optical Alignments," *56th Electronic Components and Technology Conference 2006.*

[8] M. Sindhadevi, Malathi Kanagasabai, Henridass Arun and A. K. Shrivastav, "Signal Integrity Analysis of High Speed Interconnects In PCB Embedded with EBG Structures," *J Electr Eng Technol*., vol. 11, no. 1, pp. 175- 183 , January 2016.

[9] Seung-Hwan Lee, Woo Chang Song, Jong-Myon Kim, and Jung-Rag Yoon, "Design of $(Ca0.7Sr0.3)(Zr0.8Ti0.2)O_3$-$BaTiO_3$ binary system for MLCC," *Journal of Ceramic Processing Research,* vol. 18, no. 3, pp. 188-191, January 2017.

Hwa Sun Park He received Ph.D degree in electrical engineering from Hong-ik University. Korea, 2003, respectively. He studied the electrical field mapping systems and sensor using optical signal processing at the CUOS Center at the University of Michigan in Ann-arbor 2003-2004. He worked embedded PCB technology and manufacturing at SEMCO from 2004 to 2010. His research interests are embedded PCB technology and Unique Decoupling capacitor, Optical sensor. Currently, He works as Research Fellow at Advanced Materials and Process Research Center for IT, RIC, Sungkyunkwan University.

Young il Na He received B.S, and MS, degree in electronical engineering from Kunsan University. Korea, 2002, 2004 respectively. His research interests are grahpene solution process, MEMS sensors and capacitor device. Currently, he serves as an Ph.D candidate for Sungkyunkwan Univ.

Ho Joon Choi He received B.S,, degree in electrical engine-ering from Hanseo University. Korea, 2017. His research interests are grahpene healing process and capacitor device. Currently, he serves as an M.S course for Sungkyunkwan Univ.

Su Jung Seo He received B.S, MS, and Ph.D degree in Metal material engineering from Sungkyunkwan Univ. Korea, 1981, 1983, and 1988, respectively. His research interests are Senconductior material and sensor device. Currently, he serves as a full professor for Sungkyunkwan Univ.

Dong-Hyun Baek He received his B.S., M.S., and Ph.D. degrees from Myungji Univ., Korea in 1979, 1981, and 1997, respectively. After Korean Institute of Fire Science & Engineering. He is a professor in the Dept. of Fire & Disaster Protection Engineering at Gachon Univ., Korea.

Jung Rag Yoon He received B.S, MS, and Ph.D degree in electrical engineering from Myoung Ji University. Korea, 1991, 1993, and 1999, respecttively. His research interests are dielectric material and energy storage device. Currently, he serves as an R&D Center Manager for Samwha Capacitor Co. Ltd.